USB Proceedings

2015 IEEE International Electric Machines and Drives Conference (IEMDC)

Coeur d'Alene Resort
Coeur d'Alene, ID, U.S.A.
11 - 13 May, 2015

Sponsored by

The Institute of Electrical and Electronics Engineers (IEEE)
IEEE Industrial Electronics Society (IES)

Co-sponsored by

IEEE Power and Energy Society (PES)
IEEE Industry Applications Society (IAS)
IEEE Power Electronics Society (PES)

IEEE Catalog Number: CFP15EMD-USB
ISBN: 978-1-4799-7940-0

A finite control set model predictive direct torque control for the PMSM with MTPA operation and torque ripple minimization

Qian Liu and Kay Hameyer
Institute of Electrical Machines, RWTH Aachen University, Germany
Email: Qian.Liu@iem.rwth-aachen.de

***Abstract*—In this paper, a Lyaupnov based finite control set model predictive direct torque control for the permanent magnet synchronous machine (PMSM) is proposed. In the proposed control scheme, the finite control set prediction and the Lyapunov theory are combined to minimize the torque ripple. The 8 voltage vectors of the 2-level converter are utilized as a finite control set for the torque prediction of the PMSM. A cost function considering the torque error, the Maximum Torque per Ampere (MTPA) operation and the current limitation is introduced. Comparing to the conventional finite control set predictive control, the dominant part of the cost function is utilized as a Lyapunov function to estimate the duty cycle of each voltage vector. An optimum voltage can be obtained by the optimum voltage vector from the 8 vectors and their duty cycles. A small sampling frequency and a fixed switching frequency can be realized when compared to the conventional finite set model predictive control. In the end, the simulation and experimental results validate the performance of the proposed control scheme.**

Keywords*—Current ripple, direct torque control, finite control set MPC, fixed switching frequency, Lyapunov based duty cycle, MTPA, PMSM, torque ripple.

I. INTRODUCTION

Nowadays, the PMSM is very popular in the electrical drive system in the industry due to its large torque density and high efficiency. In order to achieve a fast torque response for the PMSM, the direct torque control (DTC) is introduced as an alternative instead of the field oriented control (FOC). Compared to the FOC, the torque response with DTC is much faster since it is without the current control loop [1], [2]. The conventional DTC is realized by two nonlinear hysteresis comparators and a switching table of the converter status [2], [3]. Each of the selected converter status lasts for one sampling period of the digital controller, which results in variable switching frequency and large current and torque ripples.

In order to reduce the torque and current ripples, a revised DTC has been proposed to be combined with the space vector pulse width modulation (SVPWM) [4], [5]. A PI torque controller is introduced to calculate the voltage reference, which is implemented by the SVPWM. Therefore, the continuous voltage and constant switching frequency of the converter can be realized to reduce the current and torque ripple. However, the torque response varies depending on the gain of the PI controller [5], [6], which degrades the advantages of the DTC when compared to the FOC.

Currently, along with the development of the predictive control, numerous methods, such as the Torque Predictive Control (TPC) and the Model Predictive Control (MPC) are proposed for the torque control to achieve high performance for the PMSM. The TPC calculates the reference stator voltage for the desired torque and flux according to the torque and voltage equation of the PMSM in a predictive way [1], [6], [7]. The switching frequency of the converter is constant since the TPC is combined with the SVPWM. The torque ripple can be reduced by the TPC if a variable duty cycle of the reference stator voltage is introduced. The duty circle can be calculated in such a way that the mean torque error equals to zero in one sampling period. However, the TPC is inconvenient to consider the system constraints such as the limitation of the current and a certain level of the torque ripple remains.

For the model predictive direct torque control, a finite set of the natural voltage vectors of the inverter ((e.g. 8 voltage vectors for the 2-level inverter) is utilized as a search table to optimize the predefined cost function. One major advantage for the finite control set MPC (FCSMPC) is that a general form for the cost function can be introduced to optimize the system performance considering different system constraints [8], [9]. Therefore, a cost function considering the torque response for the PMSM can be utilized to realize the direct torque control [10], [11] and special objectives such as the MTPA condition can be taken into account [12]. However, the torque control using conventional FCSMPC has the same disadvantages as the conventional direct torque control. Each converter status lasts for one sampling period, which results in large torque and current ripples and degrades the performance of the PMSM. In order to reduce the current and torque ripple for the FCSMPC, several modifications such as quantized searching [13] and a duty cycle control [14]–[16]. With both modifications, the torque and current ripples can be reduced.

In this paper, a method for the model predictive determination of the stator voltage vector including the optimized duty cycle is introduced for the direct torque control with MTPA. The proposed scheme combines the FCSMPC and the Lyapunov theory. The cost function including the torque tracking, MTPA operation and system constraints is utilized in this paper. The dominant part of the cost function is used as a Lyapunov function to calculate the duty cycle of each voltage vector in the finite set. The FCSMPC is implemented for a revised voltage set with the calculated duty cycles. After the execution of the FCSMPC, an optimum voltage can be obtained. With a complementary voltage, the proposed

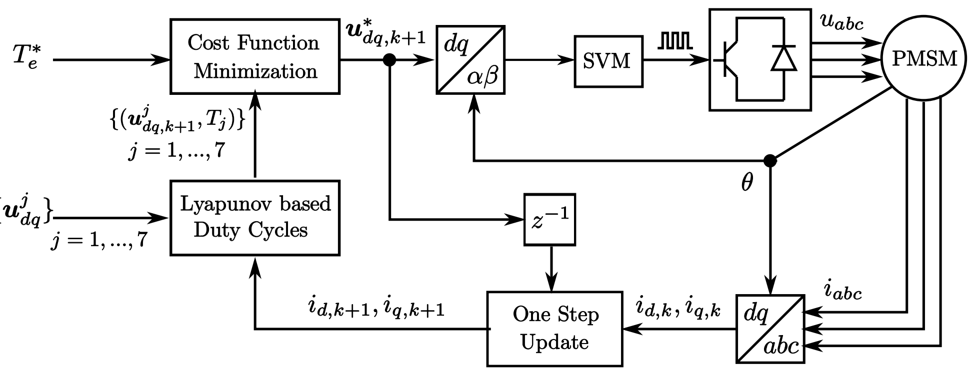

Fig. 1. Block diagram for the proposed FCSMPC strategy.

predictive control scheme has fixed switching frequency, which is realized by the SVPWM for both fast torque response and the minimization of the torque ripple.

II. PMSM AND INVERTER IN DQ REFERENCE SYSTEM

The proposed model predictive torque control is implemented in the dq reference coordinate system. The base frequency model of a PMSM described in the synchronous rotational dq coordinates is shown by the following equations:

$$\frac{di_d}{dt} = \frac{1}{L_d}(U_d - Ri_d + \omega L_q i_q), \tag{1}$$

$$\frac{di_q}{dt} = \frac{1}{L_q}(U_q - Ri_d - \omega L_d i_d - \omega \Psi_F), \tag{2}$$

$$T_e = 1.5p(\psi_F + (L_d - L_q)i_d)i_q, \tag{3}$$

where R, L_d, L_q and ψ_F are the stator resistance, inductance on d,q-axis and the magnetic flux of the PMSM respectively. p is the pole pair number. Using the Forward Euler Approximation, the discrete current model of the PMSM is described by the following equation:

$$i_{d,k+1} = (1 - \frac{TR}{L_d})i_{d,k} + \frac{T\omega L_q}{L_d}i_{q,k} + \frac{T}{L_d}u_{d,k}, \tag{4}$$

$$i_{q,k+1} = (1 - \frac{TR}{L_q})i_{q,k} - \frac{T\omega L_d}{L_q}i_{d,k} - \frac{T\omega\Psi_F}{L_q} + \frac{T}{L_q}u_{d,k}, \tag{5}$$

where T is a small time interval, which can be smaller than or equal to the sampling time T_s.

The voltage of the PMSM $\boldsymbol{u}_{dq,k} = [u_{d,k}, u_{d,k}]^T$ is realized by the inverter. A 2-level inverter has 8 different switching status that $\{(S_a, S_b, S_c) \,|\, S_{a,b,c} \in \{0, 1\}\}$, where S_a, S_b and S_c are the switching status of the three phases respectively. According to [17] and with the amplitude invariant Park transformation, the resulting voltage vectors in the dq coordinate system can be obtained by the following equation:

$$\begin{bmatrix} u_{d,k} \\ u_{q,k} \end{bmatrix} = \frac{2V_{DC}}{3}\boldsymbol{M}_k \begin{bmatrix} 1 & -\frac{1}{2} & -\frac{1}{2} \\ 0 & \frac{\sqrt{3}}{2} & \frac{\sqrt{3}}{2} \end{bmatrix} \begin{bmatrix} S_{a,k} \\ S_{b,k} \\ S_{c,k} \end{bmatrix}, \tag{6}$$

$$\boldsymbol{M}_k = \begin{bmatrix} cos\Theta_k & sin\Theta_k \\ -sin\Theta_k & cos\Theta_k \end{bmatrix}.$$

The 8 switching states 000, 001 ... 111 results in 8 voltage vectors $\{\boldsymbol{u}^j_{dq,k} \,|\, j = 0, 1, ..., 7\}$ in the dq coordinate system. Since the switchings 000 and 111 have the same voltage vector, The voltage set $\{\boldsymbol{u}^j_{dq,k} \,|\, j = 1, ..., 7\}$ is considered for the model predictive control.

III. TORQUE CONTROL WITH MODIFIED FCSMPC STRATEGY

In order to minimize the current and torque ripples for the FCSMPC torque control, a Lyapunov based FCSMPC strategy is proposed in this section. The block diagram for the proposed FCSMPC strategy is shown in fig. 1, which includes a one step update, a Lyapunov based calculation of the duty cycles for the voltage set and the optimization of the control output voltage.

A. One step update

Due to the calculation time of the digital controller, there is one step time delay between the calculation and implementation of the voltage reference. The voltage reference $\boldsymbol{u}^*_{dq,k}$ at time instant t_k is implemented to the PMSM at time point t_{k+1}. Therefore, a one step update is implemented to compensate the time delay due to the digital controller:

$$i_{d,k+1} = (1 - \frac{T_s R}{L_d})i_{d,k} + \frac{T_s\omega L_q}{L_d}i_{q,k} + \frac{T_s}{L_d}u^*_{d,k}, \tag{7}$$

$$i_{q,k+1} = (1 - \frac{T_s R}{L_q})i_{q,k} - \frac{T_s\omega L_d}{L_q}i_{d,k} - \frac{T_s\omega\Psi_F}{L_q} + \frac{T_s}{L_q}u^*_{q,k}. \tag{8}$$

The updated estimation $i_{d,k+1}$ and $i_{q,k+1}$ are utilized for the prediction process. The estimated torque $\hat{T}_{e,k+1}$ is calculated directly using equation (3).

B. Cost function for the FCSMPC

In order to achieve the torque control with MTPA condition, a cost function considering the tracking of the torque, the MTPA operation and the limitation of the current, which is similar to the one in [12], is utilized in this paper. The cost function is described by the following equations:

$$J(k+1) = \sum_{i=1}^{N_p}[k_T J_T(k+i) + k_A J_A(k+i) + k_L(J_{L1}(k+i) + J_{L2}(k+i))], \tag{9}$$

where N_p is the prediction length for the MPC, which is chosen to 1 in this paper. k_T, k_A and k_L are the weighting

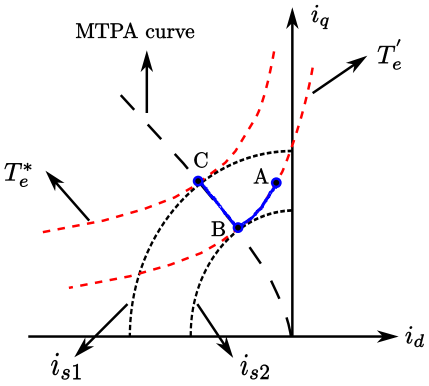

Fig. 2. Current loci of the MTPA condition.

factors of the cost function, which are positive real numbers. $J_T(k)$ and $J_A(k)$ denote the dominant objectives which are the torque dynamics and MTPA condition respectively. The description of $J_T(k)$ and $J_A(k)$ are shown by the following equations:

$$J_T(k) = (T_e^* - \hat{T}_{e,k})^2, \tag{10}$$

$$J_A(k) = (i_{d,k} + \frac{L_d - L_q}{\Psi_F}(i_{d,k}^2 - i_{q,k}^2))^2. \tag{11}$$

The current limitations of the PMSM are considerd by $J_T(k)$ and $J_A(k)$ with following description:

$$J_{L1}(k) = \begin{cases} 0 & \text{if } I_r \leq \sqrt{i_{d,k}^2 + i_{d,k}^2} \\ \left(I_r - \sqrt{i_{d,k}^2 + i_{d,k}^2}\right)^2 & \text{otherwise} \end{cases}$$

$$J_{L2}(k) = \begin{cases} 0 & \text{if } i_{d,k} \leq 0 \\ i_{d,k}^2 & \text{otherwise} \end{cases}$$

where I_r is the rated current of the PMSM. $J_{L1}(k)$ denotes the current limit due to the thermal consideration. J_{L2} is to ensure that the d-axis current i_d converges to the correct solution for the MTPA condition. With the help of the cost function, the torque control with MTPA condition is transformed to minimize the cost function $J(k+2)$.

C. Calculation of the duty cycles

In order to minimize the current and torque ripple of the PMSM with FCSMPC, a Lyapunov function is proposed to introduce a duty cycle for each voltage vector in the finite set. The proposed Lyapunov function is chosen as the dominant objectives in the cost function with $N_p = 1$, which is shown by the following equation:

$$V(k+1) = k_T J_T(k+1) + k_A J_A(k+1). \tag{12}$$

The condition $V(k+1) = 0$ denotes the desired optimum operation of the PMSM that $T_{e,k+1} = T_e^*$ and the current of the PMSM is on the MTPA curve. As shown fig. 2, $J_T(k+1) = 0$ denotes the constant torque curve and $J_A(k+1) = 0$ denotes the MTPA curve. Denoting θ and i_s as the phase angle and amplitude of the current that $i_d = -i_s sin(\theta)$ and $i_q = -i_s cos(\theta)$, the following property holds for the MTPA condition:

Lemma 3.1: Defining $f(i_d, i_q) = i_d + \frac{L_d - L_q}{\Psi_F}(i_d^2 - i_q^2)$ is a function of the current . If the torque of the PMSM is kept at a non-zero constant value, $f(i_d, i_q)$ is a strict monotonic function along the constant torque curve.

Lemma 3.1 can be easily proven by considering the variation $\frac{\partial f(i_d,i_q)}{\partial \boldsymbol{i}_{dq}}\Delta \boldsymbol{i}_{dq}$ under the constraint $\frac{\partial T_e}{\partial \boldsymbol{i}_{dq}}\Delta \boldsymbol{i}_{dq} = 0$, where $\Delta \boldsymbol{i}_{dq}$ is a current vector. With the help of Lemma 3.1, the Lyapunov function is strictly decreasing if the current trajectory is controlled as following: first along the constant torque curve until the MTPA curve $f(i_d, i_q) = 0$ is reached; then Along the MTPA curve to the operating point with $V = 0$. An example is shown in fig. 2. At the initial point A, the trajectory is along $\overrightarrow{AB}$ and $\overrightarrow{BC}$. Considering the derivative of the Lyapunov function:

$$\frac{dV(k+1)}{dt} = \frac{\partial V(k+1)}{\partial \boldsymbol{i}_{dq,k+1}} \frac{d\boldsymbol{i}_{dq,k+1}}{dt}, \tag{13}$$

where $\boldsymbol{i}_{dq,k+1}$ is the current vector. Since there exists a current trajectory so that $V(k+1)$ is decreasing, there exists $\Delta \boldsymbol{i}_{dq,k+1}$ which fulfills:

$$\frac{\partial V(k+1)}{\partial \boldsymbol{i}_{dq,k+1}} \Delta \boldsymbol{i}_{dq,k+1} \leq 0. \tag{14}$$

The equal holds if and only if the $V(k+1) = 0$ is reached. Therefore, there exists a current derivative $\frac{d\boldsymbol{i}_{dq,k+1}}{dt} = \epsilon \Delta \boldsymbol{i}_{dq,k+1}$ so that $\frac{dV(k+1)}{dt} \leq 0$ holds. Here ϵ can be a very small positive constant. Therefore, the following lemma can be easily proven:

Lemma 3.2: For each initial condition of the PMSM, if the back-emf of the PMSM is within the voltage limitation of the inverter, there exists a feasible voltage vector $\boldsymbol{u}_{dq,k+1}^*$ which fulfills $\frac{dV(k+1)}{dt} \leq 0$.

Similar to the Lemma 5.1 in [18], the following lemma also holds for the voltage vectors of the a 2-level converter:

Lemma 3.3: For the given current dynamics

$$\frac{d\boldsymbol{i}_{dq,k+1}}{dt} = \boldsymbol{A}\boldsymbol{i}_{dq,k+1} + \boldsymbol{B}\boldsymbol{u}_{dq,k+1} + \boldsymbol{E}, \tag{15}$$

if the back-emf of the PMSM is within the voltage limitation of the inverter, there exists at least one votlage vector $\boldsymbol{u}_{dq,k+1}^a$ with $a \in \{1, ..., 7\}$, which fulfills

$$\frac{V_a(k+1)}{dt} = \frac{\partial V(k+1)}{\partial \boldsymbol{i}_{dq,k+1}}(\boldsymbol{A}\boldsymbol{i}_{dq,k+1} + \boldsymbol{B}\boldsymbol{u}_{dq,k+1}^a + \boldsymbol{E}) \leq 0. \tag{16}$$

The proof of lemma 3.3 can be referred to lemma 3.2 and the proof of the Lemma 5.1 in [18].

In order to minimize the current and torque ripple of the PMSM, it is expected that the Lyapunov function stay at $V = 0$ and $\frac{dV}{dt} = 0$ in the steady state. The following calculation of the duty cycle for each voltage vector $\boldsymbol{u}_{dq,k+1}^j$ are introduced to fulfill this expectation:

$$T_{duty,k+1}^j = \begin{cases} T_\sigma & \text{if } \frac{dV_j(k+1)}{dt} > 0 \\ 0 & \text{if } \frac{dV_j(k+1)}{dt} = 0 \\ \frac{-V(k+1)}{dV_j(k+1)/dt} & \text{otherwise} \end{cases} \tag{17}$$

where T_σ is a time constant which is much smaller than the sampling time T_s. T_σ is introduced for the situation that the current limit is reached and the torque reference T_e^* can not be realized. The calculated duty cycle T_{duty}^j is limited to $[0\ T_s]$. With the help of Lemma 3.3, it can be noticed that at each time step $k+1$ without considering the current constraints, there is at least one voltage vector $u_{dq,k+1}^a$ with its duty cycle $T_{duty,k+1}^a$ to ensure the Lyapunov function $V(k{+}2) = J(k{+}2)$ to converge towards 0. On the other hand, the calculated duty cycle $T_{duty,k+1}^a$ using (17) can be used to keep $\frac{dV}{dt} = 0$ in the steady state, which will be shown in the following section. Therefore, all voltage vectors $u_{dq,k+1}^j$ with $\frac{dV_j(k+1)}{dt} < 0$ are the candidates to minimize that the cost function $J(k+2)$. Considering the case that the system constraints of the PMSM, a revised finite set $\{(u_{dq,k+1}^j, T_{duty,k+1}^j)\,|\,j = 1, 2, , 7\}$ with duty cycles is applied to the FCSMPC.

D. Implementation of the FCSMPC

To implement the FCSMPC with the revised finite set, a supplement voltage vector is defined for the control with fixed sampling rate and switching frequency:

$$\boldsymbol{u}_{dq,k+1}^s = \begin{bmatrix} Ri_{d,k+1} - \omega L_q i_{q,k+1} \\ Ri_{d,k+1} + \omega L_d i_{d,k+1} + \omega \Psi_F. \end{bmatrix}. \tag{18}$$

It can be noticed that with the supplement voltage, the derivative of the current $\frac{i_{dq,k+1}}{dt}$ is 0 so that the cost function does not change. Defining a voltage

$$\boldsymbol{u}_{dq,k+1} = (1 - T_{duty,k+1}^j)\boldsymbol{u}_{dq,k+1}^s + T_{duty,k+1}^j \boldsymbol{u}_{dq,k+1}^j. \tag{19}$$

The duration of the voltage vector $\boldsymbol{u}_{dq,k+1}$ is one sampling time T_s. When the voltage $\boldsymbol{u}_{dq,k+1}$ is applied to the PMSM, only the voltage vector $\boldsymbol{u}_{dq,k+1}^j$ with its duty cycle $T_{duty,k+1}^j$ has to be considered. The current at time point t_{k+2} with each voltage vector $\boldsymbol{u}_{dq,k+1}^j$ can be calculated by the following equation:

$$\begin{aligned} i_{d,k+2}^j =& (1 - \frac{T_{duty,k+1}^j R}{L_d}) i_{d,k+1} + \frac{T_{duty,k+1}^j \omega L_q}{L_d} i_{q,k+1} \\ &+ \frac{T_{duty,k+1}^j}{L_d} u_{d,k+1}^j, \end{aligned} \tag{20}$$

$$\begin{aligned} i_{q,k+2}^j =& (1 - \frac{T_{duty,k+1}^j R}{L_q}) i_{q,k+1} + \frac{T_{duty,k+1}^j \omega L_d}{L_q} i_{d,k+1} \\ &- \frac{T_{duty,k+1}^j \omega \Psi_F}{L_q} + \frac{T_{duty,k+1}^j}{L_q} u_{q,k+1}^j. \end{aligned} \tag{21}$$

With the predicted current, the optimum index of the voltages is obtained by evaluating the cost function:

$$b = \arg \min_{j \in \{1,\ldots,7\}} \{J^j(k+2)\}. \tag{22}$$

The optimum output reference voltage is:

$$\boldsymbol{u}_{dq,k+1}^* = (1 - T_{duty,k+1}^b)\boldsymbol{u}_{dq,k+1}^s + T_{duty,k+1}^b \boldsymbol{u}_{dq,k+1}^b, \tag{23}$$

which is realized by the SVPWM. From equation (23), it can be noticed that with the proposed FCSMPC, the optimum duty circle $T_{duty,k+1}^b$ can be T_s to minimize the cost function during the transient operation. Therefore, the torque response of the proposed strategy is as fast as the standard FCSMPC if they are using the same sampling time. On the other hand, during the steady state, the supplement voltage keeps the derivative $\frac{dV}{dt} = 0$ if $V = 0$ is reached. Therefore, the current and torque ripple can be minimized. For the proposed strategy, the derivative of the Lyapunov function has to be calculated for 7 voltage vectors for the proposed strategy. The computation time can be approximately doubled when compared to the standard FCSMPC. However, the sampling time for the proposed FCSMPC strategy can be much smaller than the standard one.

TABLE I. PARAMETERS OF THE IPMSM

Rated current	i_{max}	2.3A
Rated torque	T_{max}	1.23Nm
DC-link voltage	V_{DC}	60V
Pole pair number	p	2
Stator resistance	R	3.3Ω
d-axis inductance	L_d	16mH
q-axis inductance	L_q	20mH
Flux linkage	Ψ_F	0.0886Vs/rad

IV. SIMULATION RESULTS

The simulation model is implemented in Matlab/Simulink to validate the performance of proposed control scheme. The nominal parameters of the IPMSM are collected in Table I. The proposed control scheme is compared to the model predictive torque control with standard FCSMPC described in [12] without error rejection.

For the torque control with standard FCSMPC, the sampling frequency of the system is set to 30 kHz. The average switching frequency of the inverter is calculated by counting the number of switchings in 0.02 s and dividing by the factor 6. So the calculated switching frequency is comparable to the symmetric SVPWM. The simulation results for the torque control with standard FCSMPC and without parameter error are shown in fig. 3. It can be noticed that the switching frequency is slightly above 4 kHz. The simulation results for the torque control with proposed control strategy are shown in fig. 4. The sampling frequency of the system and the carrier frequency of the SVPWM for the proposed control strategy are both set to 4 kHz. Comparing the simulation results in fig. 3 and fig. 4, it can be noticed that both methods realize the direct torque control and the MTPA condition. The torque response with the proposed FCSMPC is slightly slower than the one with the standard FCSMPC since the sampling frequency of the proposed FCSMPC is slower. However, the current and torque ripples of the PMSM with proposed FCSMPC are minimized in the ideal case, which are much smaller than the one with standard FCSMPC.

V. EXPERIMENTAL RESULTS

To verify the feasibility of the proposed control strategy in the reality, several experiments are performed by using the PMSM with parameters from table I. The controller is implemented in the dSPACE rapid control prototyping system (DS1103). The configuration of the controller for the proposed control strategy in the experiments is set as the same as the one for the simulation in section IV. The sampling frequency for the standard FCSMPC is set to 32 kHz to achieve the switching frequency 4 kHz. The speed of the IPMSM is controlled at

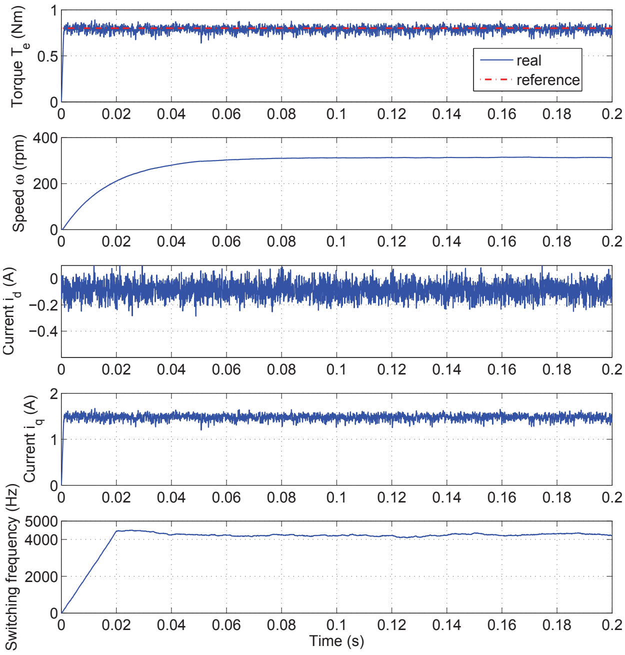

Fig. 3. Simulation results for the torque control with standard FCSMPC without parameter error.

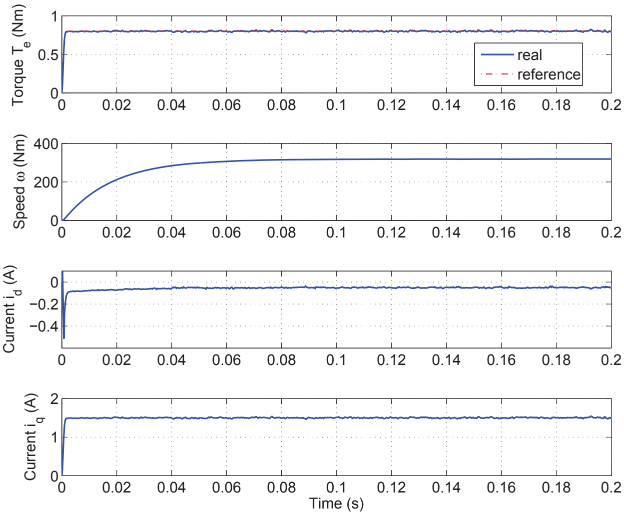

Fig. 4. Simulation results for the torque control with proposed FCSMPC without parameter error.

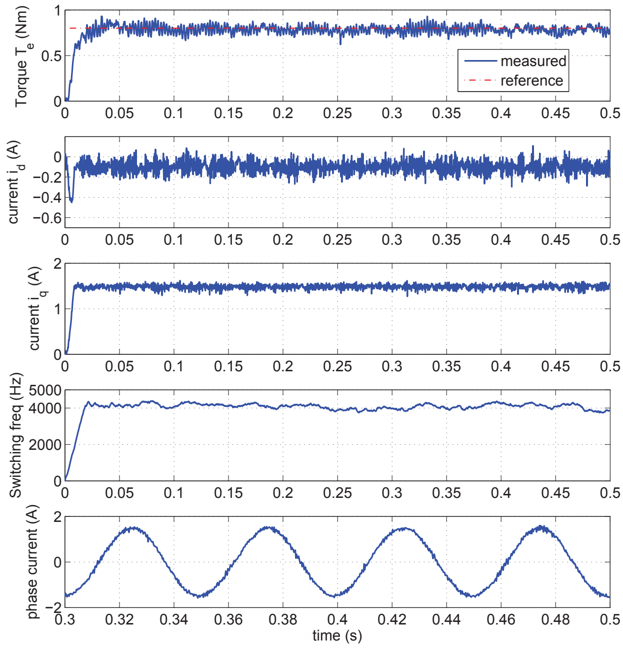

Fig. 5. Experimental results for the torque control with standard FCSMPC without parameter error.

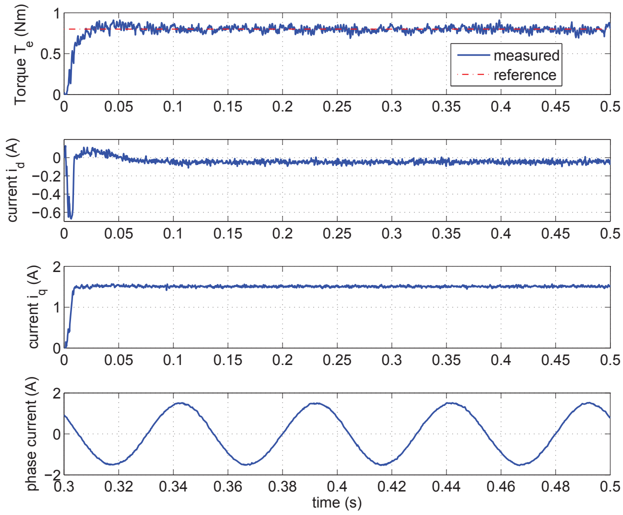

Fig. 6. Experimental results for the torque control with proposed FCSMPC without parameter error.

the speed 300 rpm by a load machine. In order to make a fair comparison, the experimental results of the standard FCSMPC are shown with the down sampling frequency 4 kHz, which is the same with the proposed one.

The experimental results without parameter error for the torque control with standard and proposed FCSMPC are shown in fig. 5 and fig. 6 respectively. It can be noticed that the torque response of the standard and proposed control strategy are approximately the same. On the other hand, with the same average switching frequency, the current and torque ripples for the proposed control strategy are much smaller than the standard one due to the introduced duty cycles.

In order to investigate the sensitivity of the parameter error for the proposed control strategy, two types parameter errors which have large influence on the PMSM stability are imposed to the experiments. The parameter errors are introduced by using the wrong parameters $1.5L_q$ and $1.3\Psi_F$ for the controller respectively. The experimental results with parameter error $1.5L_q$ are shown in fig. 7 and fig. 8. The torque control with both standard and proposed FCSMPC has approximately the same steady state operating. From the experimental results, it is shown that the L_q error has only small influence on the proposed torque control strategy. In fig. 8, the operating point deviates from the optimum MTPA condition due to the parameter error. However, the torque of the PMSM has very small displacement from the reference value. When compared to the experimental results for the standard FCSMPC in fig. 7,

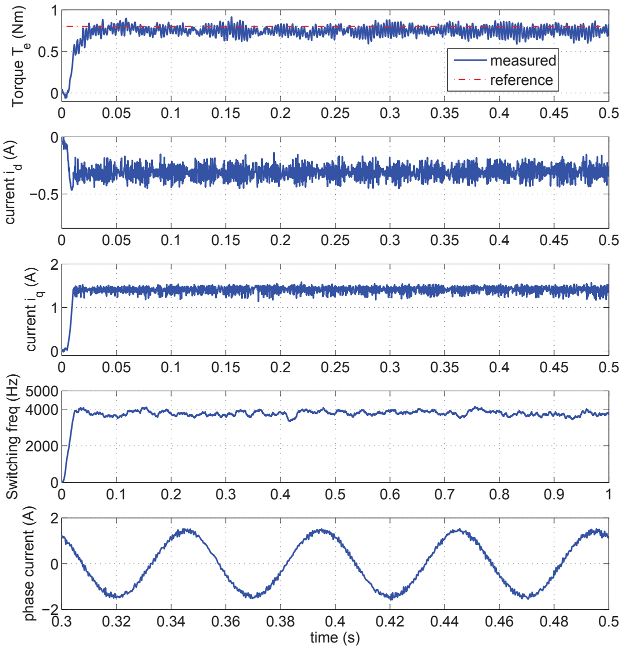

Fig. 7. Experimental results for the torque control with standard FCSMPC with parameter error $1.5L_q$.

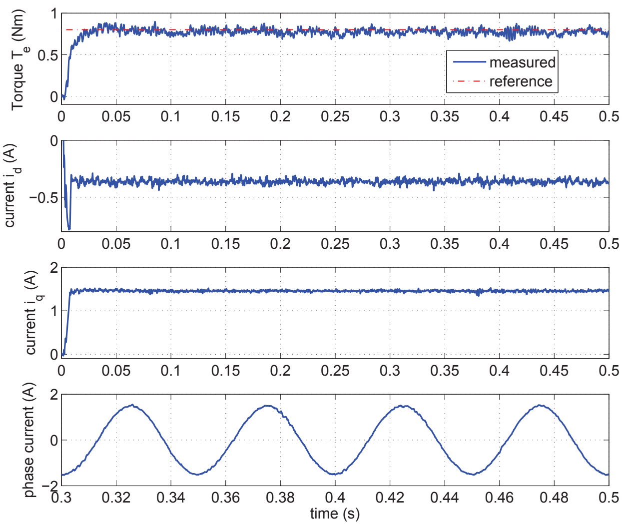

Fig. 8. Experimental results for the torque control with proposed FCSMPC with parameter error $1.5L_q$.

the current and torque ripples are still much smaller for the proposed control strategy with inductance error. On the other hand, when compared to the results for the no error case in fig. 6, the influences of the inductance error on the current and torque ripples are limited.

The experimental results with $1.3\Psi_F$ are shown in fig. 9 and fig. 10. It can be noticed that the flux error has relatively larger impact on the torque control when compared to the inductance error. In fig. 9, it can be noticed that steady state torque error exists for the proposed torque control strategy and the operating point deviates from the MTPA condition due to the flux error. However, the torque error is smaller than the one for the torque control with standard FCSMPC in fig. 10. When

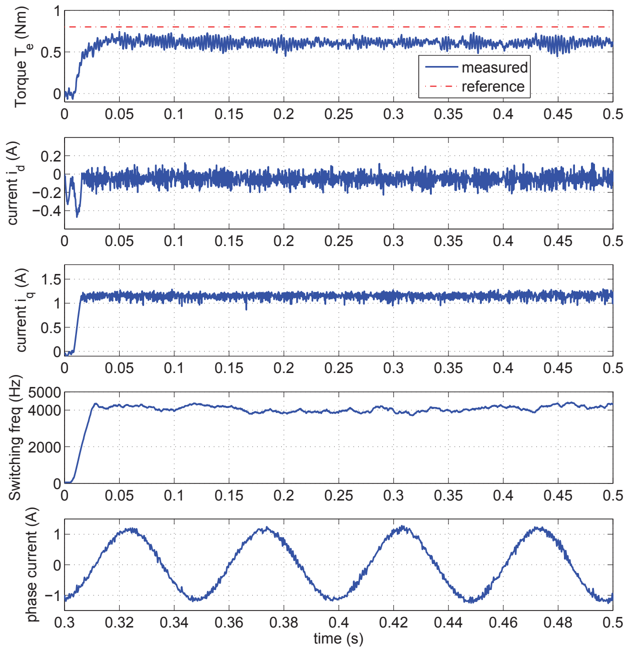

Fig. 9. Experimental results for the torque control with standard FCSMPC with parameter error $1.3\Psi_F$.

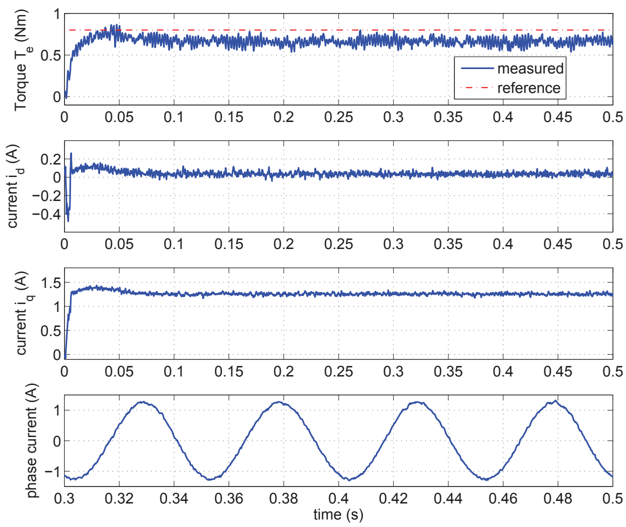

Fig. 10. Experimental results for the torque control with proposed FCSMPC with parameter error $1.3\Psi_F$.

compared to the one without parameter error in fig. 6, the torque ripple increases for the proposed control strategy, which is approximately the same as the torque ripple with standard FCSMPC in fig. 9. However, the increment of the current ripples is small for the proposed strategy with flux error, which is much smaller than the standard case. With the comparisons discussed above, it is shown that the performance of the torque control with proposed FCSMPC holds better performance than the standard FCSMPC with and without parameter errors. To increase the robustness for the proposed control scheme, it is also possible to introduce a model error compensation with Kalman or Adaptive Observer to reduce the steady state error and ripples.

VI. Conclusions

In this paper, a Lyapunov based model predictive direct torque control (FCSMPC) with MTPA for the PMSM is proposed. The natural characteristics of the 2-level converter which are the 8 voltage vectors are used to obtain an optimum voltage for the PMSM. A Lyapunov based duty cycle for each voltage vector is introduced for the implementation of the FCSMPC. A cost function including the torque tracking, the attraction of the MTPA region and the current limitation is utilized for the FCSMPC. Before the FCSMPC, the dominant part of the aforementioned cost function is used as a Lyapunov function to calculate the desired duty cycle for each voltage vector. Theoretical conclusions are shown and proved for the feasibility, stability and performance analysis of the calculated duty cycles. An optimum voltage can be obtained by combining the FCSMPC with a revised finite set of the 7 different voltage vectors with their duty cycles and a supplement voltage. The proposed control scheme can realize a small sampling frequency, fixed switching frequency and torque ripple minimization. The experimental results show the good performance of the proposed control scheme and the sensitivity of the parameter errors is investigated. The torque and current ripples can be significantly reduced when compared to the torque control with standard FCSMPC.

References

[1] H. Zhu, X. Xiao, and Y. Li, "Torque ripple reduction of the torque predictive control scheme for permanent-magnet synchronous motors," *Industrial Electronics, IEEE Transactions on*, vol. 59, pp. 871–877, 2012.

[2] M. Rahman and L. Zhong, "Comparison of torque responses of the interior permanent magnet motor under pwm current and direct torque controls," in *Industrial Electronics Society, 1999. IECON '99 Proceedings. The 25th Annual Conference of the IEEE*, vol. 3, 1999, pp. 1464–1470.

[3] G. Foo and M. Rahman, "Direct torque control of an ipm-synchronous motor drive at very low speed using a sliding-mode stator flux observer," *Power Electronics, IEEE Transactions on*, vol. 25, pp. 933–942, 2010.

[4] D. Swierczynski, M. Kazmierkowski, and F. Blaabjerg, "Dsp based direct torque control of permanent magnet synchronous motor (pmsm) using space vector modulation (dtc-svm)," in *Industrial Electronics, 2002. ISIE 2002. Proceedings of the 2002 IEEE International Symposium on*, vol. 3, 2002, pp. 723–727.

[5] L. Tang, L. Zhong, M. Rahman, and Y. Hu, "A novel direct torque controlled interior permanent magnet synchronous machine drive with low ripple in flux and torque and fixed switching frequency," *Power Electronics, IEEE Transactions on*, vol. 19, pp. 346–354, 2004.

[6] Y. Cho, K.-B. Lee, J.-H. Song, and Y. Lee, "Torque-ripple minimization and fast dynamic scheme for torque predictive control of permanent-magnet synchronous motors," *Power Electronics, IEEE Transactions on*, vol. 30, pp. 2182–2190, 2015.

[7] Y. Zhang and J. Zhu, "Direct torque control of permanent magnet synchronous motor with reduced torque ripple and commutation frequency," *Power Electronics, IEEE Transactions on*, vol. 26, pp. 235–248, 2011.

[8] P. Cortes, S. Kouro, B. La Rocca, R. Vargas, J. Rodriguez, J. Leon, S. Vazquez, and L. Franquelo, "Guidelines for weighting factors design in model predictive control of power converters and drives," in *Industrial Technology, 2009. ICIT 2009. IEEE International Conference on*, 2009, pp. 1–7.

[9] J. Rodriguez, M. Kazmierkowski, J. Espinoza, P. Zanchetta, H. Abu-Rub, H. Young, and C. Rojas, "State of the art of finite control set model predictive control in power electronics," *Industrial Informatics, IEEE Transactions on*, vol. 9, pp. 1003–1016, 2013.

[10] W. Xie, X. Wang, F. Wang, W. Xu, R. Kennel, D. Gerling, and R. Lorenz, "Finite control set-model predictive torque control with a deadbeat solution for pmsm drives," *Industrial Electronics, IEEE Transactions on*, 2015.

[11] J. Rodriguez, P. Cortes, R. Kennel, and M. Kazrnierkowski, "Model predictive control – a simple and powerful method to control power converters," in *Power Electronics and Motion Control Conference, 2009. IPEMC '09. IEEE 6th International*, 2009, pp. 41–49.

[12] M. Preindl and S. Bolognani, "Model predictive direct torque control with finite control set for pmsm drive systems, part 1: Maximum torque per ampere operation," *Industrial Informatics, IEEE Transactions on*, vol. 9, pp. 1912–1921, 2013.

[13] Z. Ma, S. Saeidi, and R. Kennel, "Fpga implementation of model predictive control with constant switching frequency for pmsm drives," *Industrial Informatics, IEEE Transactions on*, vol. 10, pp. 2055–2063, 2014.

[14] S. Wang, C. Xia, X. Gu, and W. Chen, "A novel fcs-model predictive control algorithm with duty cycle optimization for surface-mounted pmsm," in *Power Electronics, Machines and Drives (PEMD 2014), 7th IET International Conference on*, 2014, pp. 1–6.

[15] Y. Zhang and X. Wei, "Torque ripple rms minimization in model predictive torque control of pmsm drives," in *Electrical Machines and Systems (ICEMS), 2013 International Conference on*, 2013, pp. 2183–2188.

[16] Y. Zhang and S. Gao, "Simultaneous optimization of voltage vector and duty cycle in model predictive torque control of pmsm drives," in *Electrical Machines and Systems (ICEMS), 2014 17th International Conference on*, 2014, pp. 3338–3344.

[17] F. Morel, X. Lin-Shi, J.-M. Retif, B. Allard, and C. Buttay, "A comparative study of predictive current control schemes for a permanent-magnet synchronous machine drive," *Industrial Electronics, IEEE Transactions on*, vol. 56, pp. 2715–2728, 2009.

[18] G. Prior and M. Krstic, "Quantized-input control lyapunov approach for permanent magnet synchronous motor drives," *Control Systems Technology, IEEE Transactions on*, vol. 21, pp. 1784–1794, 2013.